ACCSCIENCE PUBLISHING

International Journal of Bioprinting

RESEARCH ARTICLE

Design and fabrication of a biomimetic artificial ear with enhanced mechanical properties

Sergey V. Zhirnov[1], Aleksandr A. Levin[1], Saida Sh. Karshieva[1], Vasilina A. Zakharova[1], Anzhelika-Mariia A. Burtseva[1], Stanislav V. Petrov[1], Polina A. Kovaleva[1], Khassan M. Diab[2], David N. Nazarian[2], Vyacheslav V. Vinogradov[2], Sergey S. Reshulsky[2], Anton S. Machalov[2], Natalya E. Manturova[3], Egor O. Osidak[4,5], Sergey P. Domogatsky[6], Alexey V. Kovalev[7], Vladimir A. Mironov[1], Fedor S. Senatov[1], Elizaveta V. Koudan[1]*, Yusef D. Khesuani[8], and Nikolay A. Dayhes[2]

[1]Laboratory of tissue engineering and regenerative medicine, National University of Science and Technology "MISIS", Moscow, Russia

[2]The National Medical Research Center for Otorhinolaryngology of the Federal Medico-Biological Agency of Russia, Moscow, Russia

[3]JSC Plastic Surgery and Cosmetology Institute, Moscow, Russia

[4]Imtek Ltd., Moscow, Russia

[5]Dmitry Rogachev National Medical Research Center of Paediatric Haematology, Oncology and Immunology, Moscow, Russia

[6]Laboratory of Immunochemistry, FSBI National Medical Research Centre of Cardiology Name after Academician E.I. Chazov of the Ministry of Health of the Russian Federation, Moscow, Russia

[7]Priorov Central National Institute of Traumatology and Orthopedics, Moscow, Russia

[8]Laboratory for Biotechnological Research "3D Bioprinting Solutions", Moscow, Russia

***Corresponding author:**
Elizaveta V. Koudan
(koudan1980@gmail.com)

Citation: Zhirnov SV, Levin AA, Karshieva SS, *et al.* Design and fabrication of a biomimetic artificial ear with enhanced mechanical properties. *Int J Bioprint*. 2026;12(3):026180166. doi: 10.36922/IJB026180166

Received: April 30, 2026

Revised: June 5, 2026

Accepted: June 8, 2026

Published online: June 8, 2026

Abstract

Microtia is a congenital malformation of the external part of the human ear. Recently, bioprinted auricles have been implanted in the first human patient. The remaining challenge in bioprinting of human ear is a post-implantation maintenance of bioprinted auricular construct size and shape. We hypothesize that the use of polylactide stiffeners will enable bioprinting of hybrid auricular constructs with stable post-implantation size and shape. Using the hybrid bioprinting method, auricular implants consisting of a custom-shaped polyurethane frame with polylactide stiffeners and filled with collagen hydrogel containing chondrocytes were printed. Mechanical testing of the implants was performed and it was shown that adding stiffeners to the frame increased the resistance of the structure to deformation. The implants were sutured under the temporal fascia in two mini-pigs for three months, after which a histologic and immunohistochemical study was performed. The formation of regenerated connective tissue with its own vascular network was observed, filling the entire volume of the implant. There was no evidence of inflammation or rejection. The implants maintained their size and shape after implantation. Thus, the *in vivo* evaluation of the auricular implant bioprinted by the described hybrid method gave satisfactory results in preclinical testing and the next logical step is a clinical translation.

Keywords: Cartilage implant; Bioprinting; Thermoplastic polyurethane; Polylactide; Microtia

1. Introduction

Birth defects of the external ear (auricle and external auditory canal) are called microtia.[1] Surgical correction of auricular anomalies continues to challenge plastic and reconstructive surgeons.[2] Current reconstructive material options broadly include autologous, allogeneic, or xenogeneic intercostal cartilage as grafts for ear reconstruction.[3] However, all of these materials have limitations. Autologous grafting is usually associated with inflammation, donor site pain, and a risk of pneumothorax and costochondritis.[4] Allogeneic and xenogeneic grafts have improved compliance but at a higher risk of immune rejection. An alternative to these materials is the Medpor® implant (Stryker, USA). It is a prefabricated synthetic biocompatible porous polyethylene implant that can be customized intraoperatively by heating or engraving.[5,6] The main disadvantages of Medpor® are significant risk of implant extrusion, fracture and immunogenicity.[7] Therefore, given the need to find alternatives to the above materials, cartilage tissue engineering is gradually gaining relevance in ear reconstruction research.

The concept of using tissue engineering for the treatment of microtia is one of the first targets for practical application of this technology. There are several excellent reviews on tissue engineering of auricular constructs.[8-10] At one time, mice with implanted tissue-engineered human auricles became a symbol of tissue engineering. There are two recent major trends in the development of tissue engineering of auricula: (i) bioprinting became the most popular technology;[2,11] and (ii) tissue engineered auricular constructs are already in clinical translation. At least two groups in China[12,13] and one group in USA (AuriNovo™, 3DBio Therapeutics, NCT04399239) reported the initiation of clinical trials. However, 3DBio Therapeutics terminated the study recently for reasons unrelated to safety. The clinical trial could be considered successful only in case of high level of post-implantation fidelity or long-term maintenance of implanted construct size and shape.

In our previous work,[14,15] we attempted to use printed patient-specific acellular non-biodegradable implants with biomimetic biomechanical properties. The main advantage of this approach was the low cost of the process. The main goal was not to generate cartilage, but to make the non-biodegradable implant biocompatible and biomechanically biomimetic with a high level of post-implantation fidelity. However, the polymers used induced a certain degree of unwanted foreign body reaction.

Recent advances in the development of bioprinting technology enable the biofabrication of patient-specific biodegradable tissue-engineered auricular constructs. Here, we report the novel variant of hydrid bioprinting technology using polylactide stiffener, which allows not only good level of biocompatibility and biomimetic biomechanical properties, but also high level of post-implantation fidelity demonstrated in large animals. The reported satisfactory preclinical data suggest some possible improvements and strong potential for clinical translation.

2. Materials and methods

2.1. Cell culture

We used primary cultures of porcine chondrocytes isolated from the 1.5 cm × 1.5 cm fragments of porcine cartilage after mechanical treatment and disaggregation of cartilage samples followed by incubation with 0.25% trypsin trypsin/EDTA solution (Paneco, cat. # P036p) and 200 U/mL collagenase-I solution (Gibco). The resulting suspension was filtered and transferred to a DMEM medium (Paneco, cat. # C420) containing 10% fetal bovine serum (FBS; Gibco, cat. # 16000-044), supplemented with antibiotic/antimycotic (Gibco, cat. # 15240-062), 2 mM L-glutamine (Paneco, cat. # F032), and ITS (Corning, cat.354352). The cells were incubated at 37 °C in a humidified atmosphere with 5% CO_2 and routinely split at 85%–95% confluence with trypsin/EDTA solution (Paneco, cat. # P036p).

2.2. Bioink preparation

A commercial solution of "Viscoll" sterile porcine collagen at a concentration of 40 mg/mL was used. Prior to bioink preparation, one part of the collagen solution was neutralized with four parts of DMEM containing 10% FBS and 100 mM TRIS-HCl buffer (pH 7.2–7.4) at 4 °C. The chondrocyte suspension was then added to prepare the complete bioink. The resulting composition contained 1 × 10^6 cells/mL hydrogel solution.

2.3. Bioprinting of tissue-engineered construct

A 3D model of the auricle in STL format was reconstructed from a patient's computed tomography (CT) scan data provided by the Federal Scientific Clinical Centre FMBA of Russia using the ImageJ 3D Viewer plug-in (National Institutes of Health, USA). Subsequent processing of the 3D model was performed using Fusion 360 (Autodesk, USA), and the gyroid structure was obtained using Prusa Slicer (Prusa Research, Czech Republic).

Medical grade thermoplastic polyurethane Elastollan 1170A granules (BASF, Germany) and polylactide granules (Ingeo 4032D, molecular weight 110 kg/mol, NatureWorks LLC) were used. Filaments for fused deposition modeling (FDM) printing were obtained using a HAAKE MiniLab 2 twin-screw extruder (Thermo, USA) with the following extrusion parameters: for PLA the temperature was 180 C, for TPU 170 C. Bioprinting was performed on a custom

BiZon i3 Steel printer from 3DiY, Russia with the following configuration: Cartesian kinematics with two IDEX printheads, one of which contains two direct extruders for FDM printing, the second is a syringe extruder with direct ink supply (DIW, direct ink writing). For bioprinting, the printer was placed in a NEOTERIC B2 biosafety laminar flow cabinet from Lamsystem, Russia. FDM printing parameters are as follows: layer height = 0.15 mm, line width = 0.4 mm, hot end temperature = 215 °C and 210 °C for TPU and PLA, respectively; supporting structures were printed from PLA. Hydrogel filling was performed according to the following algorithm: every five polymer layers, the pores of the gyroid mesh were filled with an equal amount of hydrogel using a syringe print head, needle diameter 0.8 mm (17G).

2.4. *In vivo* experiments

Two closely related minipigs of the *Sus salvanius* breed (FMBA, Russia) with an average weight of 37.5 kg were used to evaluate the graftability of the auricular implants. *In vivo* experiments were performed at the National Medical Research Center for Otorhinolaryngology of the FMBA of Russia and were approved by the local ethics committee (№ 04/23 от 27.11.2023). Throughout the experiment, the animals were kept in individual ventilated boxes under exhaust ventilation and were fed *ad libitum*. The animal work was carried out in accordance with the ethical principles established by the European Convention for the Protection of Vertebrate Animals used for Experimental and Other Scientific Purposes (Strasbourg, 2006) and the International Guidelines for Biomedical Research in Animals (CIOMS and ICLAS, 2012).

After the manufacture of bioengineered auricles, they were implanted under the temporal fascia. The operation was performed under total intravenous anesthesia by two teams of surgeons on both individuals. A skin incision was made in the posterior region, a flap of the temporoparietal fascia was formed on the branches of the superficial temporal artery, an auricle implant was installed and covered with a flap.

The observation period was three months, then both individuals were humanely removed from the experiment. Fragments of implants and discs were removed and fixed in a 10% neutral formalin solution on a phosphate buffer. All implanted materials were sent for histological examination.

2.5. Histological analysis

Serial 4-μm thick paraffin sections were prepared. After deparaffinization, they were stained by the Mallory method (Mallory staining, 21-032, tests, LLC "ErgoProduction") using standard techniques to detect collagen, reticular fibers, cartilage, and bone.

2.6. Immunohistochemistry

Immunohistochemical (IHC) study was aimed at detecting angiogenesis markers in the tissue sample—CD31 (PECAM-1 (platelet endothelial cell adhesion molecule-1) and vascular endothelial growth factor (VEGF), which were determined separately ("one factor at a time"). Paraffin sections were mounted on slides and deparaffinized in xylene and ethanol of different concentrations. Immunohistochemical staining was performed using an automated immunohistochemistry platform called Ventana BenchMark XT automated immunostainer (Roche) and its reagents according to the manufacturer's protocols and recommendations, using the visualization system—XT ultra View DAB v3. IHC for detection of CD31 and VEGF was performed using primary monoclonal antibodies CD31 (1A10) (Leica Biosystems) and VEGF (VG1) Dako, respectively. Positive and negative controls were used in each case. IHC results were evaluated visually by analyzing digital copies of histological slides for light microscopy. In each specimen, the staining intensity (IHC expression strength) of VEGF and CD31 was semi-quantitatively recorded by two independent observers in 5–7 adjacent fields at high magnification and scored on a scale of 0 (-, no staining detected), 1 (+, weak immunostaining), 2 (++, moderate immunostaining) to 3 (+++, strong staining). The mean score was calculated by averaging the scores and approximating the arithmetic mean to the nearest unit.

All histology slides with stained tissue sections were digitized by full scanning using a digital slide converter for the Aperio LV1 IVD microscope.

3. Results

3.1. Building a model for printing

A 3D model of a healthy human auricle was reconstructed from CT data (500 μm slice thickness) and mirrored about its base plane (Figure 1A). Figure 1B illustrates the construction of the stiffeners. The 3D model was subdivided using a series of manually selected secant planes positioned according to the anatomical features of the intact auricle: the helix, the antihelix, the concha, and the crura of the helix. In each secant plane, spline curves were created to serve as axial guides for the stiffeners. The diameter of the stiffener section ranged from 1.5 to 2.5 mm, and the final diameter of 2.0 mm was chosen based on the organoleptic characteristics of the framework.

The entire internal volume was filled with a gyroid structure using Prusa Slicer with the following parameters 70% porosity, 0 solid layers, 0 perimeters, without using sparse fill bonds. Figure 1C shows the resulting gyroid-filled

model. The gyroid structure was then combined with the stiffeners (solid-filled, formed only from perimeter lines).

Once obtained, the skeletal model (stiffening ribs together with gyroid porosity) was subtracted from the original auricle model using Prusa Slicer's built-in model combination algorithm to form the hydrogel filling region.

3.2. Hybrid bioprinting

The frame was printed under laminar conditions as follows: within each layer, the stiffener and gyroid mesh elements are printed in polylactic acid (PLA) and thermoplastic polyurethane (TPU), respectively, so that the mesh lines intersect the stiffeners, thereby increasing the strength of the stiffeners' attachment to the porous filling. Once the printing of a gyroid cell is complete, but before the gyroid angle is rotated, the pores are filled with hydrogel using a syringe extruder. After printing, the implant is carefully removed from the platform and transferred to a sterile culture medium container. The container is stored in a CO_2 incubator at 37 °C until use. Figure 2 shows the process of bioprinting of implants.

3.3. Mechanical testing of frames for resistance to membrane deformation

In order to verify the influence of the presence of the cruciform ribs on the shape retention of the implant under the tension of the skin flap, a modeling experiment was carried out by loading the skeletons with the elastomeric membrane (Figure 3). For this purpose, a testing machine was developed consisting of a fixed platform with a tensioned elastomeric membrane fixed in a ring grip, which simulates a skin flap, and a movable crosshead to which the test frame is fixed. The movable traverse was lowered onto the membrane and pressed through the implant frame, with the membrane profile image photographed from the side using a digital camera. Each frame was pressed down to a constant traverse offset from the membrane surface equal to half the ear implantation height (Figure 3A). The resulting images were binarized according to an automatically selected threshold. As can be seen in Figure 3B, the processed image contains only one central contour corresponding to the frame surrounded by the membrane. The largest contour was then found and its area value was used as a parameter associated with the retention of its 3D shape by the scaffold. An auricle model with a solid polyethylene terephthalate glycol (PETG) filling was printed as a scaffold with negligible deformation.

Three consecutive measurements were taken for each frame type. The shape retention factor S was calculated for all frame types:

$$S = \frac{s}{s_{rigid}} \quad (1)$$

where s is the measured contour area, and s_{rigid} is the contour area for the rigid frame.

Figure 3C shows that the frame labeled TPU only, consisting only of gyroid mesh, experiences the greatest

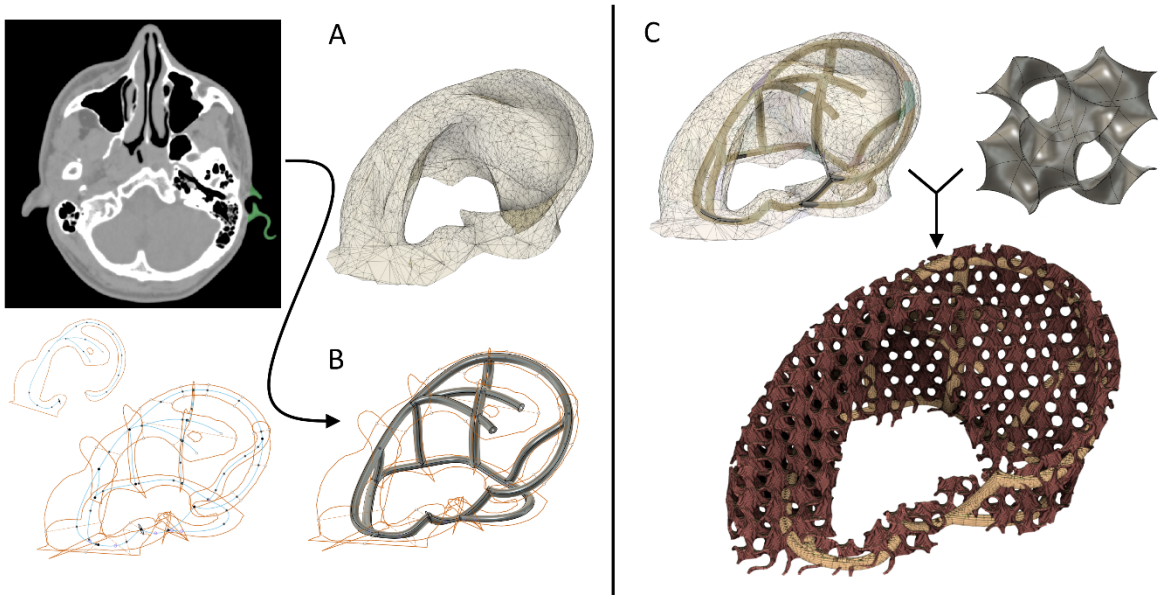

Figure 1. Designing the implant. (A) Reconstruction of a 3D model of the intact auricle from CT data. (B) Construction of stiffening ribs. (C) Formation of a porous gyroid structure with integrated stiffeners.

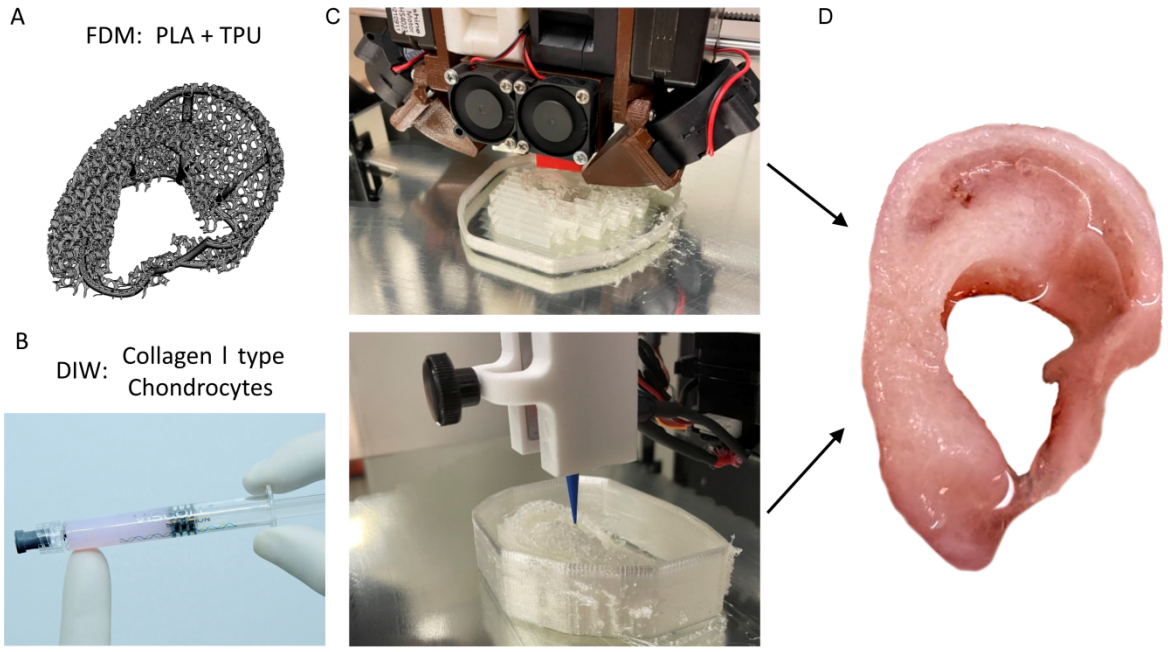

Figure 2. Bioprinting of implants. (A) Preparation of the frame model for FDM printing. (B) Preparation of bioinks. (C) Hybrid FDM/DIW 3D printing. (D) The ear-shaped implant following 3D printing and subsequent incubation in culture medium.
Abbreviations: DIW: Direct ink writing; FDM: Fused deposition modeling; PLA: Polylactic acid; TPU: Thermoplastic polyurethane.

change in shape, with a coefficient of $S = 0.5$, suggesting the possibility of significant deformation under skin flap pressure during implantation. The frame with stiffeners, TPU-PLA, deforms significantly lesser, $S = 0.72$, with the deformation increasing rapidly until the collapse of the pores above the stiffeners, which can be observed visually. This suggests that a structure with stiffeners is significantly less likely to collapse during implantation than a structure without stiffeners.

3.4. Macroscopic and histological analysis of implants

Two minipigs were implanted with the constructs under the temporal fascia (Figure 4). At 3 months after implantation, the minipigs were sacrificed, the grafts harvested and macroscopic observations made. There was no evidence of hematoma, exudate or inflammation in the surrounding tissues. All implants retained their original shape and were fully integrated with the temporal muscle and fascia. The ear-shaped chondrocyte/collagen/TPU/PLA-based implants were not deformed; the surrounding tissues adhered to their surface and replicated all their anatomical structures. Thus, we found that the TPU/PLA ear-shaped material is biocompatible and has sufficient mechanical strength to maintain its unique shape throughout the implantation period.

Hematoxylin and eosin staining of the bioengineered ears showed the distribution of fibrovascular connective tissue with blood vessels of various diameters (Figure 5A). The fibrous tissue in the collagen/TPU/PLA implant was moderately vascularized and contained rare blood-filled vessels, with the TPU implant being the least vascularized (Figure 5B and 5C). All implants contained fibroblast-like cells that formed a fibrous layer closer to the implant. Inflammatory infiltration and necrosis were not observed. Collagen fibrils were visualized using Mallory's blue combination trichrome. Collagen fibers stained more intensely in implants without cells than in implants with chondrocytes (Figure 5D and 5E). Collagen/chondrocyte/TPU/PLA-based implants contained clusters of chondrocytes, whereas individual chondrocytes were found in collagen/TPU/PLA-based implants. Connective tissue grown through TPU-only implants did not contain chondrocytes in its composition (Figure 5D–F). It is notable that immunohistochemical analysis for the expression of VEGF and CD31 T expression markers demonstrated a pronounced expression in the vascular endothelium of auricular-shaped implants. The expression of VEGF and CD31 in TPU-based implants was found to be relatively weak (Figure 5G–L).

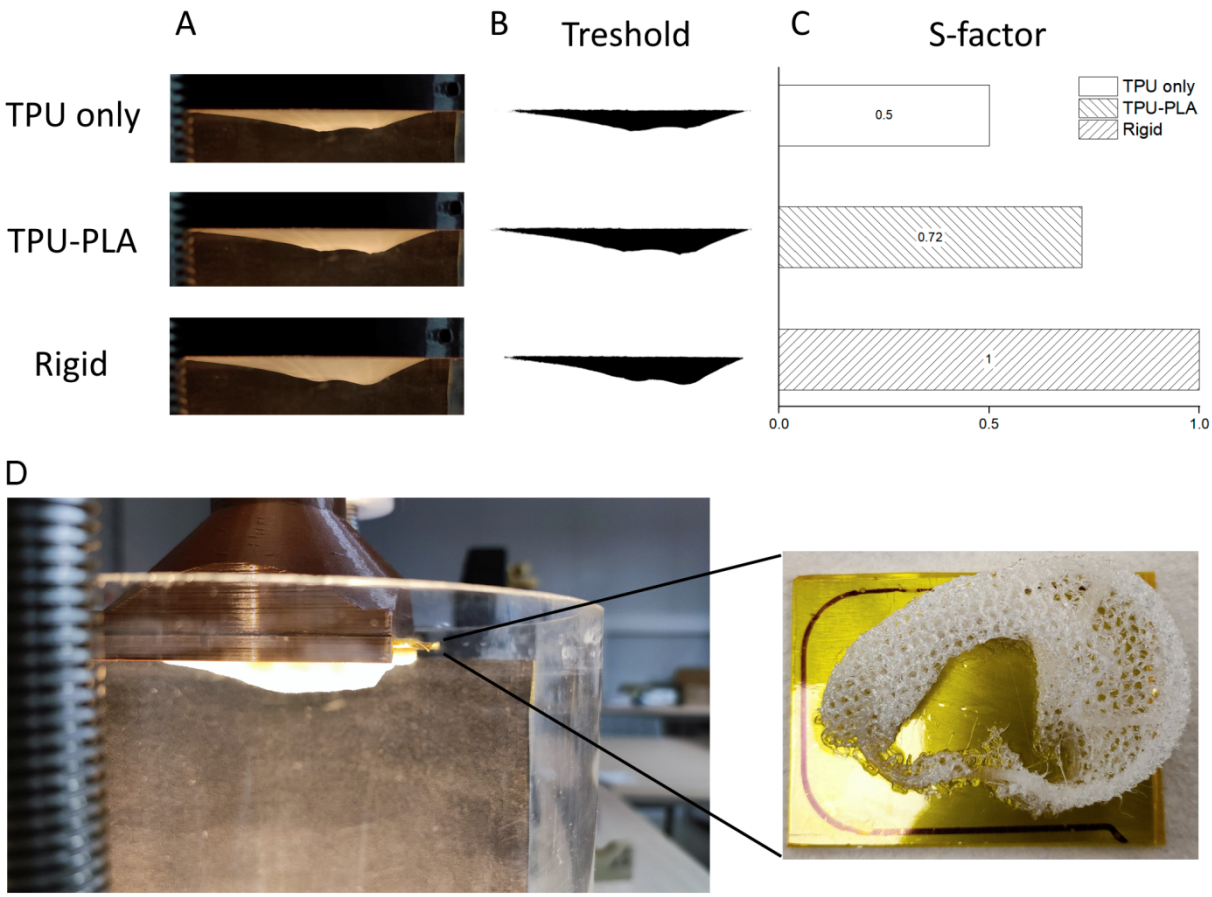

Figure 3. Testing of frames for resistance to membrane deformation. (A) Photo of a sold membrane, side view. (B) Binarized image of the membrane profile. (C) Comparison of *S*-factors for different frames. The quantitative results are presented as mean ± standard deviation (n = 3). (D) Photograph of the setup for testing of frames for resistance to membrane deformation.
Abbreviations: PLA: Polylactic acid; TPU: Thermoplastic polyurethane.

4. Discussion

There are several issues with the use of tissue-engineered auricles for the treatment of microtia: (i) tissue-engineered construct must be patient-specific or custom-designed for specific patients; (ii) tissue-engineered construct must demonstrate a high degree of post-implantation fidelity or (in other words) it must maintain its size and shape after implantation; (iii) tissue-engineered construct must not demonstrate inflammation, extensive fibrosis, or immune rejection or extensive foreign body reaction; (iv) tissue-engineered construct must be able to replace the biodegradable scaffold with extracellular matrix (ECM) produced by living cells in the tissue-engineered construct; and (v) tissue-engineered auricular construct must be able to develop into viable cartilage tissue with authentic biomechanical properties. In the reported work, we have attempted to systematically address these important issues.

Personalization of auricular implants is fundamental to achieving satisfactory aesthetic outcomes in reconstructive surgery. Recent advances in 3D bioprinting have established patient-specific fabrication as the dominant paradigm in this field.[16] Consistent with these principles, we reconstructed a 3D model of the auricle from patient's CT data and filled the printed scaffold with autologous porcine chondrocytes in a collagen hydrogel. The use of autologous auricular chondrocytes as the cell source is particularly advantageous, as these cells are programmed for elastic cartilage formation. This approach is consistent with previous reports on patient-specific auricular bioprinting. For example, Zopf *et al.*[17] fabricated patient-specific ear scaffolds using CT data and achieved good aesthetic outcomes. Our results confirm that CT-based reconstruction is a reproducible and clinically applicable method for microtia patients.

Maintaining construct size and shape after implantation

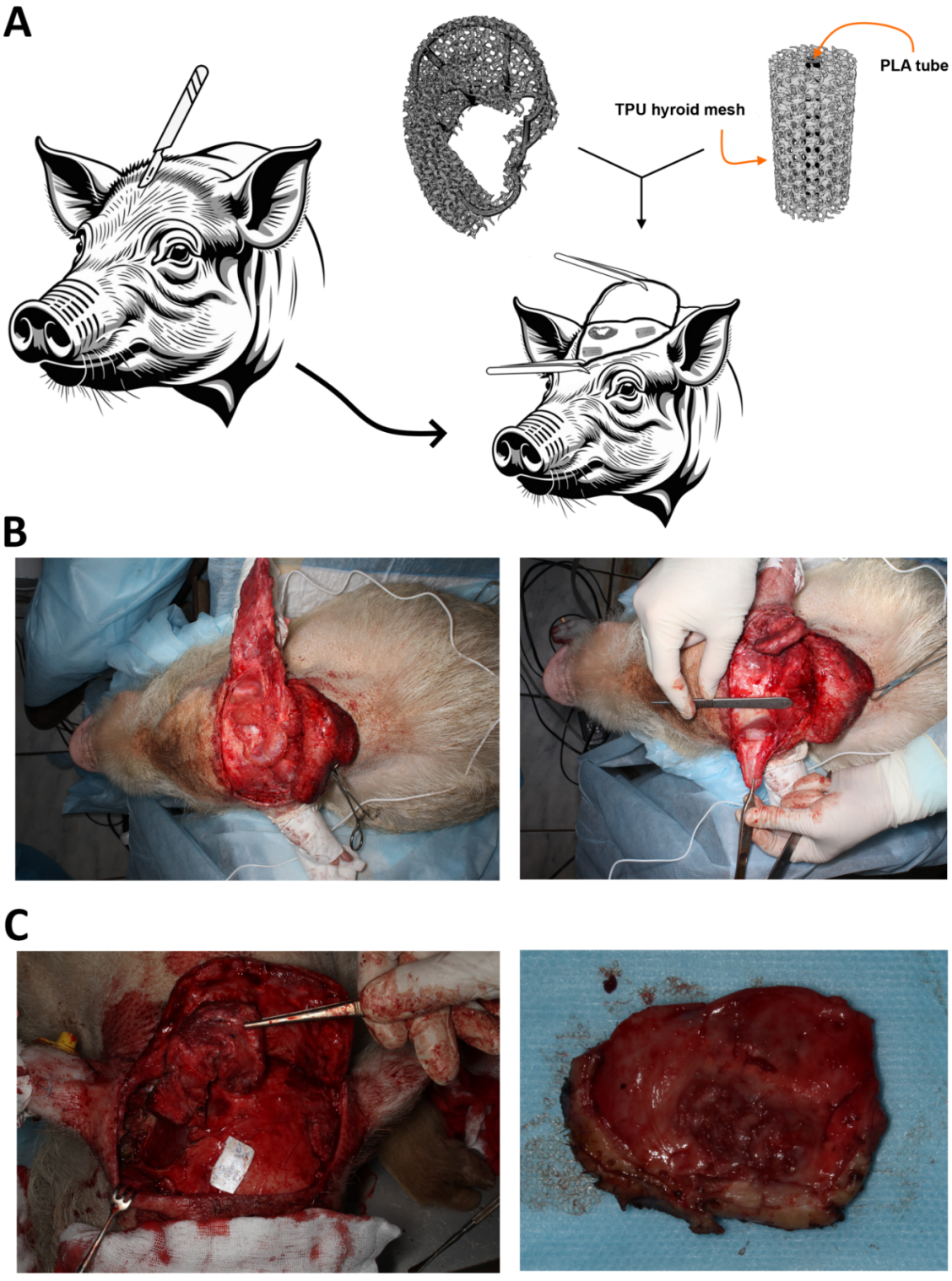

Figure 4. Experiment on grafting bioprinted constructs into minipigs. (A) Schematic diagram of the placement procedure of bioprinted grafts under the temporal fascia of minipigs. (B) Photograph of the placement procedure of bioprinted grafts under the temporal fascia of minipigs. (C) Photograph of the removal procedure of an auricular implant.
Abbreviations: PLA: Polylactic acid; TPU: Thermoplastic polyurethane.

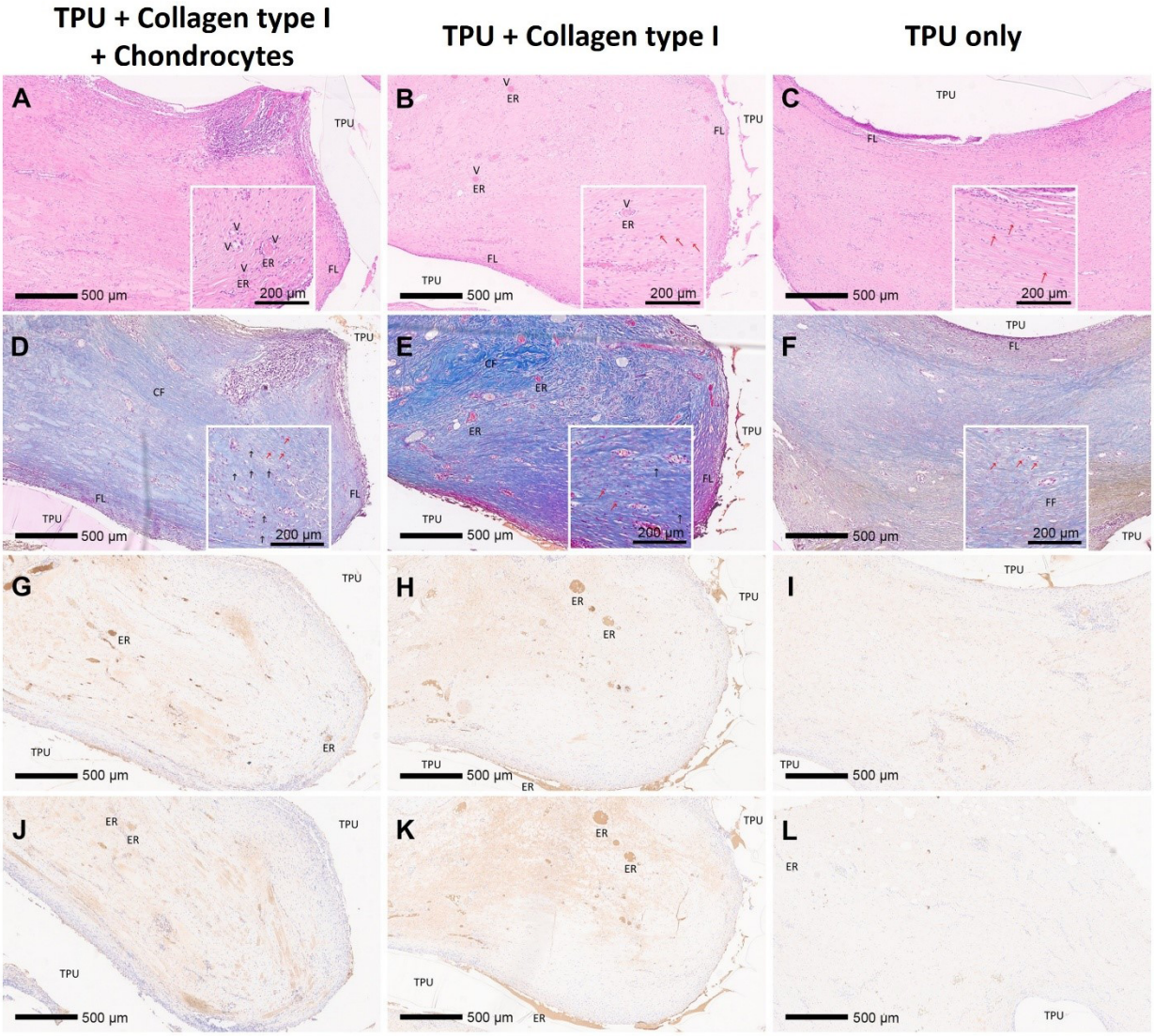

Figure 5. Histological analysis of axial sections of bioengineered implants stained with H&E (A,B,C), Mallory trichrome stain (D,E,F) and IHC staining using anti-VEGF (G,H,I) and anti-CD31 antibodies (J,K,L). (A–C) H&E sections showed the area of connective tissue with blood vessels (V) containing erythrocytes (ER) (A,B), fibroblast-like cells (red arrows) (C), and a fibrous layer (FL) around the TPU. (D–F) Mallory trichrome staining shows an abundance of collagen fibers (CF) with single rounded chondrocytes with lacunae (black arrows) and fibroblasts penetrating into the center of the implant (red arrows) and along the periphery (FL). (G–I) IHC staining for the vascular endothelial cell markers VEGF and CD31 showed angiogenic activity around the implanted constructs and within the collagen hydrogel.
Abbreviations: H&E: Hematoxylin and eosin; IHC: Immunohistochemistry; PLA: Polylactic acid; TPU: Thermoplastic polyurethane.

remains one of the most difficult challenges in auricular tissue engineering. While most of the work on ear cartilage bioprinting has focused on controlling cellular behavior by modifying both the hydrogel itself[18] and introducing bioactive components into it,[19] little attention has been paid to the problem of mechanical stability of printed scaffolds *in vivo*. In many works, the constructs intended for implantation have the simplest two-dimensional types of internal volume filling and a predominantly flat shape, which is associated with physical limitations in printing viscous gels. However, it is known that auricular implants are subject to significant mechanical stress from the pressure of the skin flap immediately after implantation,[20] which will lead to a noticeable change in the geometry of the product, which will not be able to resist this stress. In this study, we focused on solving the problem of poor mechanical stability of bioprinted ear implants. We addressed this challenge by incorporating PLA stiffeners

into a TPU gyroid scaffold. The gyroidal pore structure was chosen because of the lower anisotropy properties of printed structures made with this type of filling. At the same time, the pore structure has a considerable effect on both the vascularization of the construct and the proliferation of cells present in the hydrogel.[21] Moreover, earlier studies demonstrating that scaffold microarchitecture profoundly influences the chondrogenic potential of tissue-engineered auricular constructs. Zopf *et al.*[17] showed that defined spherical micropore architectures produce more robust cartilage formation than randomly interspersed pores, an effect attributed to differences in permeability and cell migration.

We observed that scaffolds printed from TPU alone (without stiffeners) deformed substantially under simulated skin flap compression, with a shape retention factor of only $S = 0.50$. By contrast, the TPU-PLA hybrid frames demonstrated significantly improved shape retention ($S = 0.72$). Notably, in a recent study by Fisch *et al.*,[22] which successfully engineered elastic cartilage approaching native properties, mechanical testing was limited to compression (1.1 ± 0.03 MPa), bending, and tensile moduli. The authors did not quantitatively assess dynamic shape retention under conditions mimicking post-operative skin flap compression, nor did they introduce an integrated parameter analogous to our *S*-factor. Furthermore, their approach lacks a rigid reinforcing framework, and the shape stability of the construct relies solely on the maturation of the elastic cartilage itself within a specialized bioreactor. In contrast, our TPU-PLA stiffeners provide immediate mechanical support upon implantation, which is critical for resisting compression from the overlying skin flap. To our knowledge, the present study is the first to introduce a standardized compression test that simulates postoperative pressure.

The implanted hybrid bioprinted auricular construct maintained its size and shape after implantation. It is important to mention that low post-implantation fidelity was the main problem in the first attempt to fabricate tissue-engineered auricular constructs.[23] The hybrid bioprinting approach reported here allows the successful elimination of this persistent and vexing technological problem that has undermined the potential therapeutic value of many previous attempts.[24]

The long-term success of any tissue-engineered implant depends critically on its biocompatibility. The polymers selected for our hybrid scaffold (TPU and PLA) are both well-characterized biomaterials with established safety profiles. A 2023 study investigating the *in vitro* and *in vivo* biocompatibility of 3D-printed TPU/PLA blends for tracheal scaffolds confirmed that these materials facilitate cell adhesion, migration, and proliferation while promoting angiogenesis in host cells.[25] Importantly, that study reported no significant inflammatory reaction in surrounding tissues, consistent with our own histological observations. In our 3-month minipig implantation study, we observed no evidence of hematoma, exudate, inflammation, necrosis, or foreign body giant cell formation.

The ultimate goal of auricular tissue engineering is the formation of functional elastic cartilage whose biomechanical properties approximate those of the native human ear. In our study, Mallory's trichrome staining revealed clusters of mature chondrocytes with distinct lacunae in TPU-PLA constructs containing chondrocyte-laden hydrogel, providing direct histological evidence of cartilage matrix formation. Notably, in control implants without the cell-laden hydrogel, chondrogenesis was completely absent, confirming the critical importance of the cellular component.

The living cells in the construct enabled the formation of connective tissue that regenerates with its own vascular network and fills the entire volume of the implant. Normal cartilage is a typical example of avascular tissue such as cornea or heart valves, and formation of vascular cartilage is usually evaluated as biofabrication of hypertrophic cartilage. However, the penetration of polymeric auricular implant after implantation is usually associated with suboptimal inadequate skin vascularization.[26] In this context, vascularization of bioprinted constructs allows a viability of skin-covered implants. The presence of neovascularization is critical for the safe functioning of an implanted auricular prosthesis. Since bioinert materials, such as high-density polyethylene, poorly support the ingrowth of small blood vessels into the implant, immune-competent cells are scarcely present.[27] This, in turn, can lead to severe consequences in the event of infection within the implant, for instance, due to traumatic damage to the skin. This is indirectly supported by the significantly higher rate of post-implantation removal of Medpor® (Porex Surgical, Newnan, Ga., USA) implants compared to the use of autologous cartilage in auricular reconstruction surgeries.[28] In our study, TPU-PLA constructs implanted with chondrocyte-laden hydrogel showed strong expression of VEGF and CD31, indicating active angiogenesis. Importantly, this neovascularization did not induce cartilage degradation or hypertrophy. By contrast, TPU-only constructs exhibited minimal VEGF and CD31 expression, resulting in poor tissue integration. Thus, in the context of large-volume auricular regeneration, controlled angiogenesis is not a drawback but a critical requirement for implant survival and long-term functionality.

Another interesting fact is that during embryonic chondrogenesis, regression of blood microvessels occurs before cartilage differentiation.[29] Moreover, at least theoretically, some of the endothelial cells do not die but may contribute to chondrogenesis by endothelial-mesenchymal transition.[30,31] If this is the case, then the addition of some known chondrogenic factors such as transforming growth factor beta (TGF-β)[32,33] in a bioprinted polymer or hydrogel can dramatically enhance chondrogenesis in a biomimetic manner. It could be a form of artificial biomimetic recapitulation of natural embryonic chondrogenesis.

The optimal balance between the kinetics of polymer degradation and the dynamics of *de novo* ECM synthesis by chondrocytes is responsible for maintaining the initial biomechanical properties of the bioprinted auricular construct. Acceleration and not-well-controlled polymer degradation not compensated by *de novo* synthesis of ECM could compromise initial biomechanical property of construct and even lead to low level of post-implantation fidelity or change in the construct size and shape. The balance of both processes (polymer degradation and *de novo* ECM synthesis) is essential for post-implantation fidelity and deserves special study.

Our findings have direct clinical relevance in the context of ongoing translational efforts. The AuriNovo implant (3DBio Therapeutics), evaluated in a phase 1/2 clinical trial (NCT04399239) for microtia reconstruction, demonstrated the feasibility of patient-specific bioprinted ear constructs. However, that study was recently terminated for reasons unrelated to safety. A follow-up study (NCT06072040, AUR-201) is now recruiting patients aged 8–29 years with grade II–IV unilateral microtia. Meanwhile, conventional methods remain problematic: a 2025 meta-analysis reported that porous polyethylene (Medpor®) implants are associated with higher rates of infection, framework exposure, and repeated procedures compared to autologous rib cartilage.[34] Autologous rib cartilage reconstruction, while durable, is associated with significant donor site morbidity, pneumothorax risk, and postoperative pain. Our hybrid bioprinting approach, incorporating biodegradable stiffeners and chondrocyte-laden hydrogel, addresses these limitations by providing immediate postoperative mechanical support while promoting gradual tissue regeneration, potentially reducing the need for revision surgeries.

5. Conclusion

In this study, we successfully developed a patient-specific hybrid bioprinted auricular implant that combines mechanical stability with biological integration. The implants maintained their shape and size for three months in a minipig model, with no signs of inflammation, rejection, or necrosis. Robust neovascularization and formation of fibrovascular tissue containing chondrocyte clusters were observed. These results demonstrate that the proposed hybrid implant addresses key limitations of current clinical approaches, including donor site morbidity associated with autologous rib cartilage harvesting and the high infection/exposure rates of Medpor® implants. By providing immediate mechanical support and promoting vascularization, this implant represents a promising clinical alternative for patients with microtia. The present findings demonstrate the feasibility of the proposed hybrid bioprinting approach; however, further long-term studies are warranted to assess graft maturation, post-implantation shape fidelity, and functional outcomes before clinical translation.

Acknowledgments

None.

Funding

This study was conducted under the State Assignment for Higher Education Institutions on the project "Development and Clinical Testing of Laryngeal Cartilage Implants Fabricated Using Additive Manufacturing Technologies" (project code: FSME-2026-0018).

Conflict of interest

Vladimir A. Mironov serves as an Editorial Board Member of this journal, but was not in any way involved in the editorial and peer-review process conducted for this paper, directly or indirectly. The authors declare they have no competing interests.

Author contributions

Conceptualization: Sergey V. Zhirnov, Vladimir A. Mironov, David N. Nazarian

Formal analysis: Elizaveta V. Koudan, Vasilina A. Zakharova, Anzhelika-Mariia A. Burtseva, Sergey S. Reshulsky, Polina A. Kovaleva

Funding acquisition: Yusef D. Khesuani, Natalya E. Manturova, Nikolay A. Dayhes,

Investigation: Sergey V. Zhirnov, Aleksandr A. Levin, Vasilina A. Zakharova, Saida Sh. Karshieva, Anzhelika-Mariia A. Burtseva, Alexey V. Kovalev, Egor O. Osidak, Anton S. Machalov

Methodology: Aleksandr A. Levin, Alexey V. Kovalev, Vyacheslav V. Vinogradov

Resources: Fedor S. Senatov, Sergey P. Domogatsky, Egor O. Osidak

Software: Aleksandr A. Levin, Stanislav V. Petrov
Writing–original draft: Sergey V. Zhirnov, Saida Sh. Karshieva, Elizaveta V. Koudan, Fedor S. Senatov, David N. Nazarian, Khassan M. Diab
Writing–review and editing: Elizaveta V. Koudan, Yusef D. Khesuani, Vladimir A. Mironov

Ethics approval and consent to participate

Animals experiments have been approved by the local ethics committee of the National Medical Research Center for Otorhinolaryngology of the FMBA of Russia (№ 04/23 from 27.11.2023).

Consent for publication

Not applicable.

Availability of data

Data are available from the corresponding author upon reasonable request.

References

1. Reinisch JF, Tahiri Y, eds. *Modern Microtia Reconstruction*. Cham, Switzerland: Springer Nature Switzerland AG; 2019.

   doi: 10.1007/978-3-030-16387-7

2. Huang Y, Zhao H, Wang Y, *et al*. The application and progress of tissue engineering and biomaterial scaffolds for total auricular reconstruction in microtia. *Front Bioeng Biotechnol*. 2023;11:1089031.

   doi: 10.3389/fbioe.2023.1089031

3. Bhamare NC, Tardalkar KR, Kshersagar J, *et al*. Tissue engineered human ear pinna derived from decellularized goat ear cartilage: clinically useful and biocompatible auricle construct. *Cell Tissue Bank*. 2022;23(1):43-55.

   doi: 10.1007/s10561-021-09911-1

4. Reighard CL, Hollister SJ, Zopf DA. Auricular reconstruction from rib to 3D printing. *J 3D Print Med*. 2018;2:35-41.

   doi: 10.2217/3dp-2017-0017

5. Ali K, Trost J, Truong T, Harshbarger R. Total ear reconstruction using porous polyethylene. *Semin Plast Surg*. 2017;31(3):161-172.

   doi: 10.1055/s-0037-1604261

6. Jiang C, Zhao C, Chen B, *et al*. Auricular reconstruction using Medpor combined with different hearing rehabilitation approaches for microtia. *Acta Otolaryngol*. 2021;141(6):572-578.

   doi: 10.1080/00016489.2021.1900601

7. Zhang B, Zeng X, Yang X. Clinical applications of ear reconstruction with Medpor [in Chinese]. *Zhong Nan Da Xue Xue Bao Yi Xue Ban*. 2019;44(5):562-570.

   doi: 10.11817/j.issn.1672-7347.2019.05.014

8. Otto IA, Melchels FP, Zhao X, *et al*. Auricular reconstruction using biofabrication-based tissue engineering strategies. *Biofabrication*. 2015;7(3):032001.

   doi: 10.1088/1758-5090/7/3/032001

9. Bichara DA, O'Sullivan NA, Pomerantseva I, *et al*. The tissue-engineered auricle: Past, present, and future. *Tissue Eng Part B Rev*. 2012;18(1):51-61.

   doi: 10.1089/ten.teb.2011.0326

10. Bhamare N, Tardalkar K, Khadilkar A, Parulekar P, Joshi MG. Tissue engineering of human ear pinna. *Cell Tissue Bank*. 2022;23(3):441-457.

    doi: 10.1007/s10561-022-09991-7

11. Lee JS, Kim BS, Seo D, Park JH, Cho DW. Three-dimensional cell printing of large-volume tissues: application to ear regeneration. *Tissue Eng Part C Methods*. 2017;23(3):136-145.

    doi: 10.1089/ten.TEC.2016.0362

12. Zhou G, Jiang H, Yin Z, *et al*. In Vitro regeneration of patient-specific ear-shaped cartilage and its first clinical application for auricular reconstruction. *EBioMedicine*. 2018;28:287-302.

    doi: 10.1016/j.ebiom.2018.01.011

13. Su XH, Ye J, Lei C, *et al*. Secondary ear reconstruction based on the Nagata method after unsatisfactory microtia surgery outcomes. *J Plast Reconstr Aesthet Surg*. 2023;87:251-258.

    doi: 10.1016/j.bjps.2023.10.075

14. Karalkin PA, Gryadunova AA, Pereira FDAS, *et al*. Morphological analysis of in vivo biocompatibility of printed auricle prosthesis. *Morfologiia*. 2017;152(6):61-66.

    doi: 10.17816/morph.398192

15. Kasyanov VA, Pereira FDAS, Parfenov VA, *et al*. Development and implantation of a biocompatible auricular prosthesis. *Biomed Eng*. 2016;49(6):327-330.

    doi: 10.1007/s10527-016-9559-5

16. Ovsianikov A, Yoo J, Mironov V, eds. *3D Printing and Biofabrication*. Cham, Switzerland: Springer International Publishing AG; 2018.

    doi: 10.1007/978-3-319-45444-3

17. Zopf DA, Flanagan CL, Mitsak AG, Brennan JR, Hollister SJ. Pore architecture effects on chondrogenic potential of patient-specific 3-dimensionally printed porous tissue bioscaffolds for auricular tissue engineering. *Int J Pediatr Otorhinolaryngol*. 2018;114:170-174.

    doi: 10.1016/j.ijporl.2018.07.033

18. Visscher DO, Lee H, van Zuijlen PPM, *et al*. A photo-crosslinkable cartilage-derived extracellular matrix bioink for auricular cartilage tissue engineering. *Acta Biomater*.

2021;121:193-203.

doi: 10.1016/j.actbio.2020.11.029

19. Jia L, Hua Y, Zeng J, *et al*. Bioprinting and regeneration of auricular cartilage using a bioactive bioink based on microporous photocrosslinkable acellular cartilage matrix. *Bioact Mater*. 2022;16:66-81.

doi: 10.1016/j.bioactmat.2022.02.032

20. Wei Y, Li L, Xie C, *et al*. Current Status of Auricular Reconstruction Strategy Development. *J Craniofac Surg*. 2024;35(3):984-992.

doi: 10.1097/SCS.0000000000009908

21. Silva C, Pais A, Caldas GAR, Gouveia B, Alves JL, Belinha J. Study on 3D printing of gyroid-based structures for superior structural behavior. *Prog Addit Manuf*. 2021;6(4):689-703.

doi: 10.1007/s40964-021-00191-5

22. Fisch P, Kessler S, Ponta S, *et al*. Tissue Engineered Human Elastic Cartilage From Primary Auricular Chondrocytes for Ear Reconstruction. *Adv Funct Mater*. 2026;36:e30253.

doi: 10.1002/adfm.202530253

23. Brennan JR, Cornett A, Chang B, *et al*. Preclinical assessment of clinically streamlined, 3D-printed, biocompatible single- and two-stage tissue scaffolds for ear reconstruction. *J Biomed Mater Res B Appl Biomater*. 2021;109(3):394-400.

doi: 10.1002/jbm.b.34707

24. Cohen BP, Bernstein JL, Morrison KA, Spector JA, Bonassar LJ. Tissue engineering the human auricle by auricular chondrocyte-mesenchymal stem cell co-implantation. *PLoS One*. 2018;13(10):e0202356.

doi: 10.1371/journal.pone.0202356

25. Abdul Samat A, Abdul Hamid ZA, Jaafar M, Ong CC, Yahaya BH. Investigation of the In Vitro and In Vivo Biocompatibility of a Three-Dimensional Printed Thermoplastic Polyurethane/Polylactic Acid Blend for the Development of Tracheal Scaffolds. *Bioengineering*. 2023;10(4):394.

doi: 10.3390/bioengineering10040394

26. Joshi A, Choudhury S, Gugulothu SB, Visweswariah SS, Chatterjee K. Strategies to Promote Vascularization in 3D Printed Tissue Scaffolds: Trends and Challenges. *Biomacromolecules*. 2022;23(7):2730-2751.

doi: 10.1021/acs.biomac.2c00423

27. Später T, Menger MD, Laschke MW. Vascularization strategies for porous polyethylene implants. *Tissue Eng Part B Rev*. 2021;27(1):29-38.

doi: 10.1089/ten.TEB.2020.0077

28. Ma Y, Lloyd MS. Systematic Review of Medpor Versus Autologous Ear Reconstruction. *J Craniofac Surg*. 2022;33(2):602-606.

doi: 10.1097/SCS.0000000000008130

29. Hallmann R, Feinberg RN, Latker CH, Sasse J, Risau W. Regression of blood vessels precedes cartilage differentiation during chick limb development. *Differentiation*. 1987;34(2):98-105.

doi: 10.1111/j.1432-0436.1987.tb00055.x

30. Wu M, Zhang JD, Tang RN, *et al*. Elevated PTH induces endothelial-to-chondrogenic transition in aortic endothelial cells. *Am J Physiol Renal Physiol*. 2017;312(3):F436-F444.

doi: 10.1152/ajprenal.00210.2016

31. Zhang J, Wang L, Cao H, *et al*. Neurotrophin-3 acts on the endothelial-mesenchymal transition of heterotopic ossification in rats. *J Cell Mol Med*. 2019;23(4):2595-2609.

doi: 10.1111/jcmm.14150

32. Futrega K, Robey PG, Klein TJ, Crawford RW, Doran MR. A single day of TGF-β1 exposure activates chondrogenic and hypertrophic differentiation pathways in bone marrow-derived stromal cells. *Commun Biol*. 2021;4(1):29.

doi: 10.1038/s42003-020-01520-0

33. Wang W, Rigueur D, Lyons KM. TGFβ signaling in cartilage development and maintenance. *Birth Defects Res C Embryo Today*. 2014;102(1):37-51.

doi: 10.1002/bdrc.21058

34. Finestone SA, Ortiz-Ocasio LS, Shetty A, *et al*. Rib Autograft Versus Porous Polyethylene Implant Outcomes in Microtia Reconstruction: A Meta-Analysis and Systematic Review. *Cleft Palate Craniofac J*. 2026;63(6):1667-1676.

doi: 10.1177/10556656251349274